



UNIVERSITAT
POLITÈCNICA
DE VALÈNCIA



INSTITUTO DE INGENIERÍA DE
ALIMENTOS PARA EL DESARROLLO

STUDY OF FREEZING PROCESS IN PORK LOIN (*LONGISSIMUS DORSI*) BY THERMOGRAPHY AND DIELECTRIC SPECTROSCOPY

MÁSTER EN CIENCIA E INGENIERÍA DE LOS ALIMENTOS
ESPECIALIDAD EN DIRECCIÓN Y GESTIÓN DE LA INDUSTRIA
ALIMENTARIA

Student: Encarnación Hinarejos Gómez

Academic directors: Pedro J. Fito Suñer

Marta Castro Giráldez

Nuria Balaguer Cuenca

Institute: Instituto Universitario de
Ingeniería de Alimentos para el Desarrollo

STUDY OF PORK MEAT FREEZING PROCESS BY INFRARED THERMOGRAPHY AND DIELECTRIC SPECTROSCOPY

Hinarejos, E., Balaguer, N., Castro-Giráldez, M.; Fito, P.J.

RESUMEN

Actualmente, el proceso de congelación es un método ampliamente utilizado en la industria cárnica con el fin mantener el valor nutricional y las características organolépticas de los productos cárnicos. El objetivo del presente trabajo de investigación fue implementar y validar métodos de control no destructivos que permitiesen controlar los fenómenos fisicoquímicos que se producen durante la etapa de congelación, pudiendo evaluar así el impacto final de dicha operación en un sistema complejo como es la carne. Para ello, se siguió la evolución de la operación de congelación en lomo de cerdo (*Longissimus Dorsi*) con una cámara termográfica PI OPTRIS® 160 (OPTRIS GmbH, Berlín, Alemania) cuyo rango espectral de longitud de onda (λ) se encuentra comprendido entre 7,5 y 13 μm . Los resultados obtenidos permitieron demostrar la existencia de un gradiente de potencial químico que provocó un flujo de agua desde el interior hacia el exterior del sistema. A su vez, como resultado de los fenómenos de nucleación y por ende de la influencia de la tensión superficial existente, se generó un gradiente de potencial químico que provocó la atracción de moléculas de agua, dando lugar a la generación de aglomerados de hielo y a la deshidratación progresiva del tejido. Estos fenómenos, produjeron cambios significativos en la señal beta (Efecto Maxwell-Wagner) y en la región microondas del espectro electromagnético. Dichas alteraciones en el espectro sirven como base para establecer un método de control del proceso de congelación así como del estado y la estructura del tejido muscular en un producto cárnico.

Palabras clave: congelación, espectro electromagnético, infrarojos, microondas, potencial químico, producto cárnico, radiofrecuencia, tensión superficial.

RESUM

Actualment, el procés de congelació és un mètode àmpliament utilitzat en la indústria càrnia per tal de mantenir el valor nutricional i les característiques organolèptiques dels productes carnis. L'objectiu del present treball de recerca va ser implementar i validar mètodes de control no destructius que permeteren controlar els fenòmens fisicoquímics que es produeixen durant l'etapa de congelació, podent avaluar així l'impacte final d'aquesta operació en un sistema complex com és la carn. Per allò, es va seguir l'evolució de l'operació de congelació en llom de porc (*Longissimus dorsi*) amb una

càmera termogràfica PI OPTRIS ® 160 (OPTRIS GmbH, Berlín, Alemanya) amb un rang espectral de longitud d'ona (λ) comprès entre 7,5 i 13 μm . Els resultats obtinguts van permetre demostrar l'existència d'un gradient de potencial químic que va provocar un flux d'aigua des de l'interior cap a l'exterior del sistema. Al mateix temps, com a resultat dels fenòmens de nucleació i per tant de la influència de la tensió superficial existent, es va generar un gradient de potencial químic que va provocar l'atracció de molècules d'aigua, donant lloc a la generació d'aglomerats de gel i a la deshidratació progressiva del teixit. Aquests fenòmens, van produir canvis significatius en el senyal beta (efecte Maxwell-Wagner) i a la regió microones del espectre electromagnètic. Aquestes alteracions en l'espectre serveixen com a base per establir un mètode de control del procés de congelació i de l'estat i l'estructura del teixit muscular en un producte carni.

Paraules clau: Congelació, espectre electromagnètic, infrarojos, microones, potencial químic, producte carni, radiofreqüència, tensió superficial.

ABSTRACT

Frozen storage is a method widely implemented in meat industry in order to maintain the nutritional value and sensorial characteristics of meat products. The aim of this research was to implement and validate non-destructive control techniques that allow the monitoring of the physicochemical phenomena occurred during the freezing stage. This enables to evaluate the final impact of this operation in a complex system such as meat. To do this, the evolution of the freezing process in pork loin (*Longissimus dorsi*) was followed by a thermographic camera Optris PI® 160 thermal imager (Optris GmbH, Berlin, Germany), whose spectral infrared range of wavelength (λ) is comprised between 7.5 and 13 μm . The results obtained have demonstrated the existence of a chemical potential gradient which caused a flux of water from the middle to the lateral of the system. In turn, as a result of nucleation phenomena and the influence of the surface tension existent, a chemical potential gradient was caused, leading to the attraction of water molecules. This provoked the generation of ice agglomerations and the progressive tissue dehydration. These phenomena generated significant changes on the beta signal (Effect Maxwell-Wagner) and on the microwave range of the electromagnetic spectrum. Those variations serve as the basis for establishing a control method of the freezing process and the state and the structure of the muscle tissue within meat products.

Key words: Chemical potential, electromagnetic spectrum, freezing, infrared, meat product, microwave, radiofrequency, surface tension.

1. INTRODUCTION

Freezing is an important preservation method used for extending the shelf life of meat and meat products since compared with other methods; it leads to a minimal loss of quality during long-term storage at low temperatures (Soyer *et al.*, 2010). From an engineering point of view, the freezing process is an unsteady-state heat transfer phenomenon in which the food loses heat by convection through its surface and by conduction at its interior (Rahman *et al.*, 2008). The most important factor affecting the freezing process is food composition, where the water content, the characteristic of other food components, soluble and insoluble solids; and other factors such as specific heat, enthalpy and coupled transport phenomena of mass and energy are important (Jie *et al.*, 2003). Additional influencing aspects are food microstructure, particle size, porosity and certain biological aspects like species, age and maturity (Devine *et al.*, 1996; Hamdami *et al.*, 2004).

More specifically, the freezing process consist of freezing, frozen storage and thawing. Freezing involves lowering the product temperature generally to -18°C or below (Fennema *et al.*, 1973). The temperature reduction process can be divided into three distinct phases: a pre-cooling or chilling phase in which the material is cooled from its initial temperature to the freezing point temperature (T_f), a phase change period which represents the crystallization of most of the water; and a tempering phase in which the product reaches the final established temperature (eg: -18°C).It is noteworthy that typical cooling curves show at the beginning of process an abrupt rise in temperature due to liberation of the heat of fusion after an initial supercooling. This stage represents the onset of ice crystallization. Once the crystal embryos exceed the critical radius for nucleation, the system nucleates and releases its latent heat faster than the heat removed from the system. The temperature then increases instantly to the initial freezing temperature (T_f) (Rahman & Driscoll, 1994; Rahman, 1999; Rahman *et al.*, 2008) in order to start the period in which most of the ice formation occurs.

The main advantage of modelling the freezing process is to contribute to understand the complex changes motivated by the variations of temperature and the changes in the quantity and availability of water in a food system. It also assists in identifying food's stability during storage as well as in selecting a suitable condition for processing (Rahman, 2006).

Food engineers are interested in predicting cooling and freezing times in order to estimate the refrigeration requirements for freezing systems and to design the necessary equipment for effective and rational processing (Delgado & Sun, 2001). Minimization of the energy requirement, reliability safety and quality of the product must also be considered. Models available to describe the freezing process can be divided into two main groups: heat transfer models and coupled heat and mass transfer models. A good number of studies of coupled heat and mass transfer have included experiments for either establishing the control of physical properties for analysis or to validate multi-convective diffusion models (Glodstein *et al.*, 2010). Nonetheless, despite the progress made in the modelling of freezing, there is still a large gap in the field of modern thermodynamics. Indeed today there are no

conclusive studies to control simultaneously both, the transport phenomena and the phase and structural changes produced as consequence of the application of a heat treatment.

Being able to develop a thermodynamic model in the meat industry, in order to describe the physicochemical phenomena during freezing, is intrinsically related to the implementation of on-line control methods that ensure an adequate shelf life of the product. In this sense, nowadays in the meat industry the use of two cutting-edge technologies for the processing control is promoted: the dielectric spectroscopy and the thermal imaging (TI).

Dielectric spectroscopy determines the dielectric properties of a medium as a function of frequency. It is based on the interaction of an electric external field with the sample (Metaxas & Meredith, 1993; Nelson & Datta, 2001); complex permittivity (ϵ_c) is the dielectric property that describes this interaction (Metaxas & Meredith, 1993; Nelson & Datta, 2001). The real part of complex permittivity is called dielectric constant (ϵ') and the imaginary part is called loss factor (ϵ''). Most of the investigations in meat are focused on detecting the phase or compositional changes that occur as a result of heating. The reason is based on the fact that most of the water in muscle is held by capillary action by the myofibrils. When the muscle is heated, proteins denature, shorten and expel the entrapped juice. The release of water and dissolved ions, mainly calcium and magnesium, into the extracellular spaces should cause a detectable change in the dielectric properties. Nevertheless, there are no studies to monitor changes in meat during freezing. Despite this, research done in fish demonstrates the suitability of this technique for controlling the freezing stage (Clerjon & Damez, 2007; Kent *et al.*, 2004; Kent *et al.*, 2000; Lougovois *et al.*, 2003; Barassi *et al.*, 1981; Hoffmann, 1981; Lupin *et al.*, 1980; Damoglou, 1980; Burt *et al.*, 1976).

With regard to the infrared thermography technique aforementioned, note that it is an excellent method to study the heat transfer in multicomponent systems such as the meat muscle. TI is a technique that converts the radiation emitted by a body surface into temperature data without establishing contact with the object (Vadivambal & Jayas, 2011). The infrared radiation emitted by a body surface contains characteristic information of the material composition and its properties (Giorleo & Meola, 2002). The use of this information through an appropriate system of data acquisition and treatment allows determining and controlling certain properties which are difficult to measure otherwise. In fact, due to the enormous potential of the infrared thermography as a tool of control and design (Gowen *et al.*, 2010), the food industry is investing effort and money to adapt it to different processing lines, especially in the agriculture sector (Alchanatis *et al.*, 2006; Chaerle & Van der Straeten, 2000; Lamprecht *et al.* 2002; Stajnko *et al.*, 2004; Fito *et al.*, 2004; Sugiura *et al.*, 2007; Oerke *et al.*, 2006).

Regarding the applicability of this technique in meat industry, several studies have shown that it is feasible to use the TI for the assessment of pork and raw ham quality (Costa *et al.*, 2007) as well as for determining and controlling the evolution of the internal temperature of cooked chicken meat (Ibarra *et al.*, 1999; Ibarra *et al.*, 2000; Ibarra *et al.*; 2000). The aim of this

work is to determine the effect of internal water flux in meat freezing process and evaluate the use of infrared and dielectric techniques to control the meat freezing process.

2. MATERIALS AND METHODS

2.1 Experimental procedure

Experiments were carried out using five loins (*Longissimus dorsi*) collected at 6 hours post-mortem from the slaughterhouse “La cope” placed in Torrente, Valencia. Prior to freezing, several samples were extracted from each loin in order to undertake a preliminary analysis based on the raw meat quality characterization ($\text{pH}_{24\text{h}}$, $L_{24\text{h}}^*$ value and drip loss), moisture and water activity measurements and dielectric properties analysis in the microwave and radiofrequency range. Concurrently, a DSC study was made in order to calculate the specific heat of meat during the freezing process. Finally, a microstructural study was performed by Low-temperature scanning electron microscopy (Cryo-SEM) either in fresh and frozen samples. An experimental flow chart of the conducted research is shown in Figure 1. Once the sampling was done, every sample was properly labelled, sealed with parafilm and kept at 4°C in an incubator Hotcold-M (JP Selecta®) until the corresponding analysis were made.

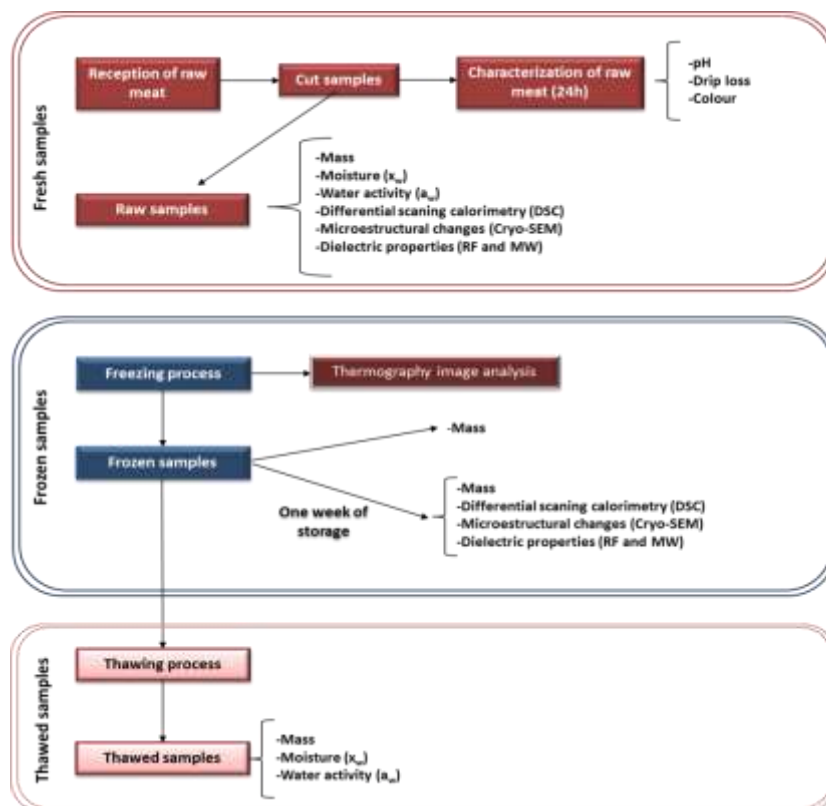


FIGURE 1. Flow chart of the experimental procedure.

Pork loins, were classified based on $\text{pH}_{24\text{h}}$, $L_{24\text{h}}^*$ value and drip loss, according to the classification shown in Table 1 (Toldrá & Flores, 2000). The pH of samples was measured through a punch pH-meter S-20 SevenEasy™ (Mettler Toledo, Spain) at 24 h after slaughtering. Drip loss determination was undertaken following the method proposed by Honikel (1998). The colour of samples was measured through the surface reflectance spectra in a spectrophotometer Minolta CM-3600D (Minolta Co. Ltd., Japan) at 24 h post-mortem. The colour coordinates CIE $L^*a^*b^*$ (CIE, 1978) were instrumentally calculated based on D65 illuminant and 10° observer. Water content was determined by drying at 110°C at atmospheric pressure, following the ISO 1442 (1997), for meat products. Finally, the surface water activity (a_w) was determined by a dew point hygrometer Decagon (Aqualab®, series 3 TE), with precision $\pm 0,003$. Measurements were made in structured samples (not minced), thus a_w obtained is considered to be surface a_w . All the measurements were made in triplicate.

TABLE 1. Meat classification based upon $\text{pH}_{24\text{h}}$, drip loss and $L_{24\text{h}}^*$ coordinate.

Meat quality classes	$\text{pH}_{24\text{h}}$	Dripp Loss (%)	$L_{24\text{h}}^*$
Pale Soft Exudative (PSE)	-	≥ 6	> 56
Red Firm Non exudative (RFN)	< 5.8	< 6	50-56
Dark Firm Dry (DFD)	$> 5,8$	< 3	< 50

2.2 Freezing process and thawing

2.2.1 FREEZING

Two cylindrical meat samples of six centimetres of diameter and 10 centimetres in height were extracted from each loin in perpendicular to the direction of fibres. Prior to the freezing of samples, masses were registered by a precision balance Mettler Toledo AB304-S (± 0.001). Freezing was performed at -20°C in a chest freezer with forced air circulation (Model. ACR-45/87, Dycometal, S.L, Barcelona, Spain) at a cooling rate of $0.1^\circ\text{C}/\text{min}$ for 245 min (See Figure 2). An infrared camera Optris PI® 160 thermal imager (Optris GmbH, Berlin, Germany) was placed into an extruded polystyrene insulation sheet (68x52x4) (Chovafoam type 4I, Leroy Merlin, S.L, Valencia, Spain) that served as the lid of the freezer. This set-up was located approximately at 20 cm of the sample surface. The camera was connected directly to a computer so that the whole process could be recorded on-line. A certified emissivity label of 25 mm diameter ($\epsilon=0.95$) (Optris GmbH, Berlin, Germany) was used as a reference emitter to calculate the reflected energy received by the infrared camera. The evolution of temperature during freezing was controlled by 4 K-thermocouples connected to an Agilent 34972A data acquisition system (Agilent Technologies, Malaysia). Thermocouples were properly placed on the certified emissivity label, the

aluminium strip, the meat surface and the freezer; latter in order to determine the room temperature. Once the centre of the samples reached an internal temperature of -18°C , the mass of the samples was registered. Following, the meat cylinders were stored for a week, in a conventional freezer (Model SJ-P6M-WH, Sharp, Spain) at -18°C .

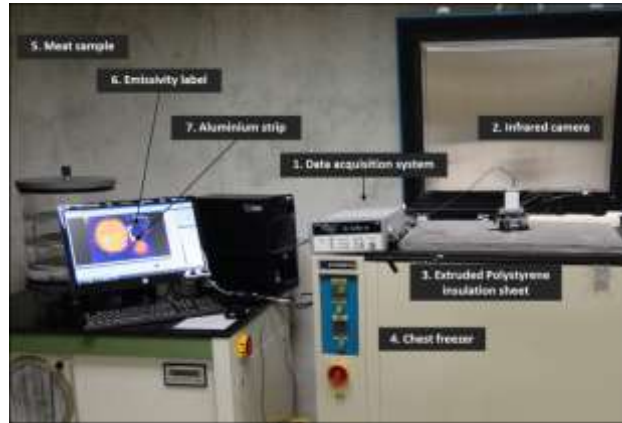


FIGURE 2. Experimental set-up. 1) Data acquisition system, 2) Infrared camera, 3) Extruded Polystyrene insulation sheet, 4) Chest freezer with air forced air circulation, 5) Meat sample, 6) Certified emissivity label ($\epsilon=0.95$).

2.2.2 THAWING

After one week of storage, frozen meat samples were cut in order to obtain samples of proper dimensions for the dielectric and microstructural study. The remaining sample of each meat cylinder was thawed in an incubator Hotcold-M(JP Selecta®) during 48 hours at 4°C . After this time, moisture and water activity analysis were determined in triplicate.

2.3 Thermography analyses

Thermal images were acquired using the Optris PI® 160 thermal imager (Optris GmbH, Berlin, Germany). It uses a two-dimensional Focal Plane array with 160×120 pixels, a spectral range of $7.5\text{-}13\ \mu\text{m}$, resolution of 0.05°C and an accuracy of $\pm 2\%$. The camera covers a temperature range of -20 to 100°C . It has a field of view of $23^{\circ} \times 17^{\circ}$ with a minimal focus distance of $0.02\ \text{m}$. The camera is supported by the software Optris PI Connect (Optris GmbH, Berlin, Germany). In this study, the software was used for compensating the acquired thermal images in relation to emissivity, acquiring on-line thermal measurements on the meat samples and converting the thermal images to an appropriate format for image processing. A certified emissivity material ($\epsilon = 0.95$) by Physikalisch-Technische Bundesanstalt (PTB) was used to correct the sample emissivity.

2.4 Dielectric properties

2.4.1 RADIOFREQUENCY RANGE

The system used to measure dielectric spectra at low frequencies consists of an Agilent 16451B parallel plate fixture connected to an Agilent 16451B impedance analyzer (Figure 3). The electrode B of the fixture, which has a 5 mm guard electrode, was used. The diameter of the samples used was 46 mm and the thickness was determined individually for each meat sample with an accuracy of ± 0.01 mm. The thickness of the samples was in the range 2–4 mm due to the limitations in the slicing system. Preliminary experiments demonstrated that, in this thickness range, the dielectric properties of each loin do not present significant differences. The Contacting Electrode Method (Rigid Metal Electrode) was used. This method consists of setting the sample between the electrodes, ensuring good contact between the electrodes and the sample. The dielectric properties were measured by performing an OPEN/ SHORT correction. Dielectric spectra of meat samples were measured in perpendicular to fibre direction. The frequency range of the measurements was from 40 Hz to 4 MHz.

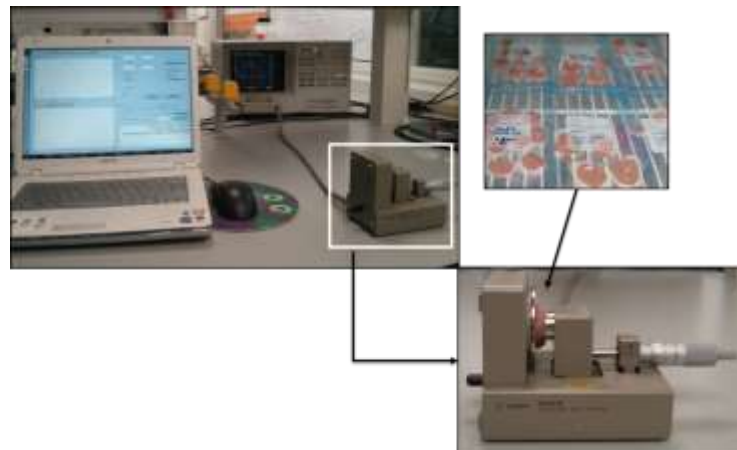


FIGURE 3. Equipment for measuring meat dielectric properties which consists on an agilent 16451B parallel plate fixture connected to an agilent 16451B impedance analyzer. Meat samples preparation can also be appreciated.

2.4.2 MICROWAVE RANGE

The system used to measure dielectric properties consists of an Agilent 85070E open-ended coaxial probe connected to an Agilent E8362B Vector Network Analyzer. The software of the Network Analyzer calculates the dielectric constant and loss factor as a reflected signal function. Calibration was performed by using three different types of loads: air, short-circuit and 4°C Milli-Q water. All determinations were registered from 500 MHz to 20 GHz following the direction of fibres.

2.5 Phase transitions

Specific heat of meat throughout freezing was calculated using a differential scanning calorimeter Mettler Toledo DSC 1 (Mettler Toledo, Spain) provided with the full range temperature sensor FRS5. The calibration of the equipment was performed by the automatic calibration function FlexCal supplied by the manufacturers. Samples of around 15-20 mg were enclosed in hermetically sealed aluminium pans (Mettler Toledo, ME-00026763) and then loaded onto the equipment at room temperature. An empty hermetically sealed pan was used as the reference sample.

In this research three different scans were performed. Firstly, fresh samples were heated from 15 to 115°C at a heating rate of 10°C/min in order to evaluate the initial protein state within meat muscle. A second scan was set with the aim to reproduce two cycles of freezing and thawing. To do this, four stages were programmed. In every stage samples were cooled from room temperature to -20°C at 5°C/min and heated next from -20°C to room temperature. Finally, a third scan was applied to frozen samples for evaluating the ice formation and the influence of freezing process in proteins state. Every scan was performed in triplicate.

Once the scans were finished, analyses of the samples were carried out by the STARe software fitted with the DSC equipment. The crystallization and melting peaks were characterized by the onset, endset, peak temperature and enthalpy involved in the transitions.

2.6 Analyses of microstructural changes: Low-temperature scanning electron microscopy (CryoSEM).

Microstructure of fresh and frozen samples was analyzed by CryoSEM. A CryoACryostage CT-1500C unit (Oxford Instruments, Witney, UK), coupled to a Jeol JSM-5410 scanning electron microscope (Jeol, Tokyo, Japan), was used. The sample was immersed in slush N₂ (-210°C) and then quickly transferred to the Cryostage at 1 kPa where sample fracture took place. The sublimation (etching) was carried out at -95°C. The final point was determined by direct observation in the microscope, working at 5 kV. Then, once again in the Cryostage unit, the sample was coated with gold in vacuum (0.2 kPa), applied for 3 min, with an ionization current of 2 mA. The observation in the scanning electron microscope was carried out at 15 kV, at a working distance of 15 mm and a temperature $\leq -130^\circ\text{C}$.

3. RESULTS

3.1 Raw material characterization

In the present study, the classification of the raw meat was undertaken according to the values obtained for L* coordinate, drip loss and pH analysis

at 24 hours postmortem as explained in section 2.1 of materials and methods. Table 2 shows the classification of the five loins used:

TABLE 2. Meat classification based upon pH_{24h}, drip loss and L_{24h}* coordinate.

Loin	pH ₂₄	Driploss (%)	L* _{24h}	Quality classification
Loin 1	5,627 ± 0,006	3,4 ± 0,3	51,36 ± 0,07	RFN
Loin 2	5,67 ± 0,04	4,77 ± 0,10	52,5 ± 0,9	RFN
Loin 3	5,68 ± 0,02	5,0 ± 0,6	51,9 ± 0,4	RFN
Loin 4	5,677 ± 0,006	5,4 ± 0,3	54,4 ± 0,5	RFN
Loin 5	5,640 ± 0,010	2,76 ± 0,03	53,2 ± 0,4	RFN

As it can be observed, all the loins were classified as RFN, indicating therefore that the results obtained in this study are not influenced by variations in the quality of meat.

3.2 Infrared thermography: Emissivity estimation

All the objects with temperature above the absolute zero emit thermal radiation following the Planck law. In the present study, the infrared camera registered the thermal flux energy emitted by different bodies inside the freezer; the camera estimates the temperature of the surfaces by using the Stefan-Boltzmann equation. In this case, the emissivity value used for registering the temperatures by the IR camera was. Due to the fact that the emissivity of the bodies is changing with the freezing treatment, the temperatures obtained by the camera is not real, and thus, the temperatures were converted into thermal flux energies, which can be considered as the response of the pyrosensor of the camera to the radiant energy in the infrared spectrum. The radiant energy that can be absorbed by the pyrosensor corresponds to the energy emitted by the superior orbital of the molecules that compound the surfaces of the bodies. The overall flux energy received by the camera can be defined by equation 1:

$$E_T = \varepsilon_S \sigma T_S^4 = F \cdot \varepsilon_{obj} \sigma T_{obj}^4 + (1 - \varepsilon_{sur}) \sigma T_{sur}^4 - (1 - \tau_{air}) F \cdot \varepsilon_{obj} \sigma T_{obj}^4 + E_{Ch} \quad (1)$$

Where E_T is the overall flux energy received by the pyrosensor (W/m^2), F is the geometric factor, being 1 because the meat surface was located in parallel with the camera, ε is the emissivity (dimensionless; from the object, surroundings or fixed in the camera), σ the constant of Stefan-Boltzmann ($5.67 \cdot 10^{-8} W/m^2 K^4$), T the temperature (K), being the subindexes: "obj" emitting object, "sur", emitting surroundings, "air" properties of air and "S" are the data obtained from the IR camera; E_{Ch} is the energy emitted in a first order transition or chemical reaction. First term represents the energy flux emitted by the meat sample; the second term is the energy flux emitted by the surroundings and the third term represents the energy flux absorbed by the air. Latter was negligible due to the short distance between the sample and the camera.

To obtain the sample emissivity it was necessary to determine the energy flux emitted by the surroundings. It was estimated by using a reference

material with known emissivity ($\epsilon = 0.95$) The following equation was used for this purpose:

$$E_T^{ref} = 0.95 \cdot \sigma \cdot T_{ref}^4 + E_{sur} \quad (2)$$

Where, E_T^{ref} is the overall energy flux of the reference material registered by the IR camera (W/m^2) and T_{ref}^4 is the temperature of the reference material registered with a K-thermocouple (K). The energy flux emitted by the surroundings was calculated with equation 2 and subtracted from the energy flux emitted by the meat sample, which was registered by the IR camera.

The emissivity of meat was calculated for the whole freezing process from the energy flux emitted by the sample and the temperature registered by the K-thermocouples, (Figure 4). Next, the emissivity obtained was used for obtaining the whole profile of temperatures (Figure 5).

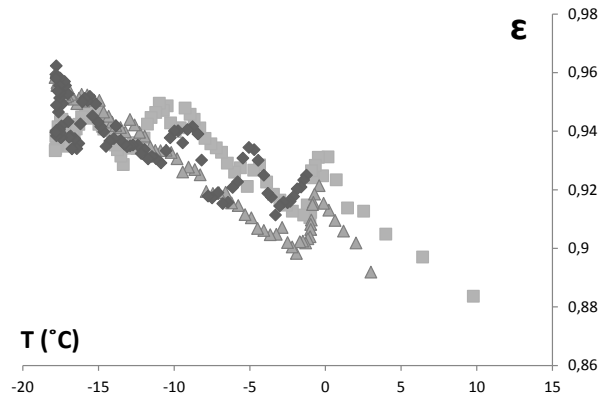


FIGURE 4. Evolution of corrected emissivity with the temperature of the meat samples, where: loin 2 (■), loin 3 (◆), loin 5 (▲).

3.3 Freezing profiles and thermodynamic approach

Once the emissivities were estimated in the temperature range of freezing, it was possible to obtain the temperature profiles during the process. The following figure (see Figure 5) shows the temperature profiles at different freezing times.

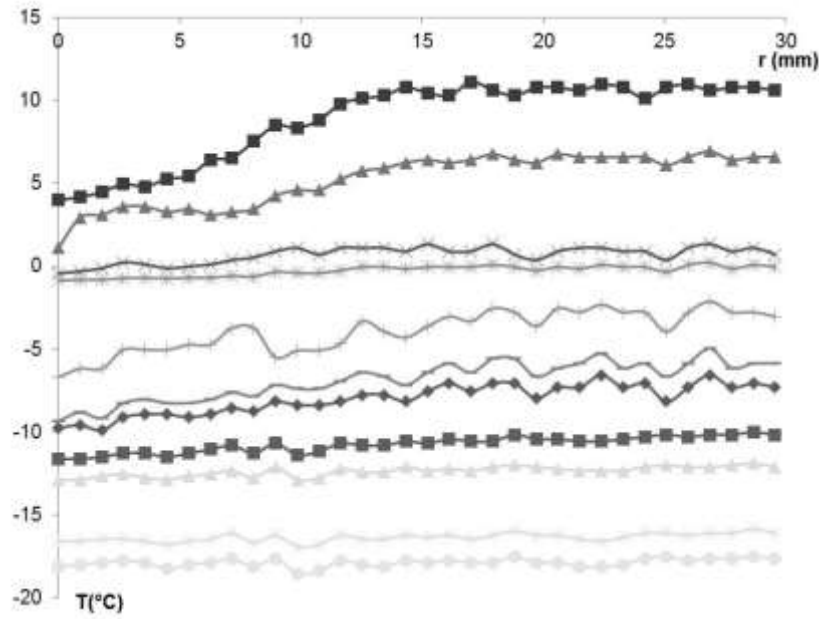


FIGURE 5. Temperature profile of pork loin during freezing process as a function of distance (r), considering 0 the lateral. Being (➕) 3min; (➔); 6 min; (➡) 9 min; (➞) 24 min; (⏏) 60 min; (—) 87 min; (➤) 93 min; (⏏) 111 min; (➞) 144 min; (⏏) 204 min; (➞) 246 min.

In figure 5 it is possible to observe how the freezing begins at the lateral of the sample and progresses toward the middle of the piece. Freezing process produces a concentration of liquid phase decreasing the melting temperature. A gradient of water chemical potential appears promoting a water flux from the middle to the lateral, heating the sample in the direction of the water flux. This water flux is promoted by the production of ice and the consequent concentration of the liquid phase. These phenomena decrease the water activity of the sample.

The water activity of meat through the freezing can be estimated by Robinson & Stokes (1965) adapted by Fontan and Chirife (1981), which it is shown in the following equation (see equation 2):

$$-\ln(a_w) = 9.6934 \cdot 10^{-3} \cdot \Delta T_f + 4.761 \cdot 10^{-6} \cdot \Delta T_f^2 \quad (2)$$

Being ΔT_f the gradient between the initial freezing temperature and the freezing temperature of the product. While the system produces ice and concentrates the liquid phase, the melting temperature decreases, approaching this system to a subcooling system.

The engine of the water movement is the gradient of water chemical potential (μ_w), being this water chemical potential defined as follows (Castro-Giráldez *et al.*, 2011):

$$\mu_w = \mu_w^0 + RT \ln a_w - s \cdot T + v \cdot P \quad (3)$$

Where, a_w is the water activity, s is the partial entropy, v is the partial volume and P is the absolute pressure.

Furthermore, the gradient of water chemical potential in sense of radio may be estimated as follows:

$$\frac{\partial \mu_w}{\partial r} = RT \frac{\partial \ln(a_w)}{\partial r} - s \frac{\partial T}{\partial r} + v \frac{\partial P}{\partial r} \quad (4)$$

Where the entropy can be estimated from the heat exchanged. In this case, the variation of pressure can be negligible.

$$s = \frac{q}{T} = \frac{C_p \cdot \rho \cdot V \cdot \Delta T}{T} = C_p \cdot \rho \cdot \pi r^2 \cdot L \cdot \frac{\Delta T}{T} \quad (5)$$

Being L the length of the cylinder (10 cm), V the variation of volume in the direction of the flux, ΔT the increment of temperature, ρ the density of meat (1082 kg/m^3) and C_p the specific heat ($0,41 \pm 0,1 \text{ J/kg}^\circ\text{C}$) obtained by DSC. Heat (q) is estimated as internal energy variation (ΔU).

Figure 6 shows the evolution of the water chemical potential during the freezing process at three different positions from the middle to the lateral of the sample estimated by finite elements analysis. The first hundred minutes, the water chemical potential is higher in the lateral and lower in the middle of the cylindrical sample. As figure 6 shows, the water chemical potential is maximum and positive at 50 min, this phenomenon attracts water molecules. However, simultaneously the water chemical potential at 10 mm from the lateral is maximum but negative, causing repulsion of water molecules. In the middle, the water chemical potential is the lower. After 100 min, there are continuous changes and fluctuations in the sense of flux in the whole profile. Therefore, in this case the water chemical potential does not explain all the water motion of the sample and another mechanism is required to estimate the unexplainable deviation in the water flux by the increase of the free energy.

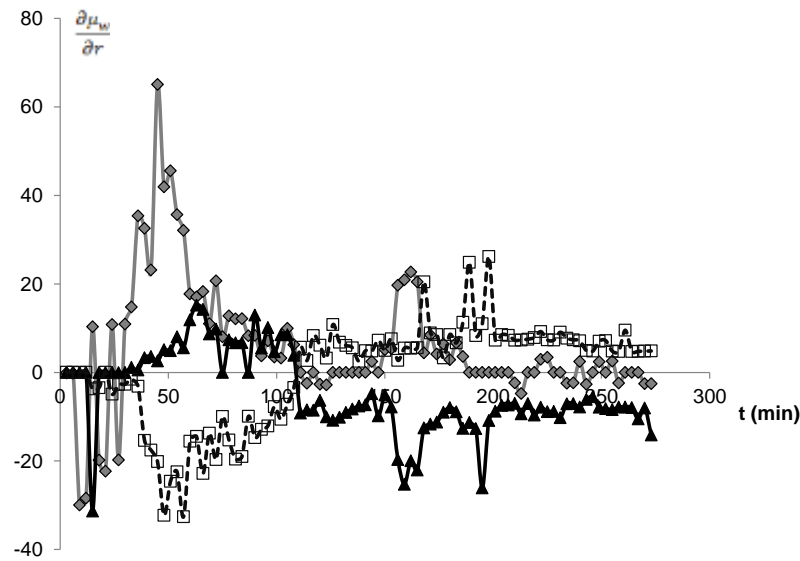


FIGURE 6. Evolution of water chemical potential (J/mol) throughout time at (▲) the middle, (□) 10 mm from the lateral and (◆) the lateral.

When the ice crystals appear, the high surface tension of ice agglomeration produces a new term in the water chemical potential, and the power of this mechanism (surface tension) increases with the growth of the ice agglomeration because it is a surface behaviour.

The new term of water chemical potential may be estimated as follows (Rusanov, 2005):

$$\left. \frac{\mu_w^\sigma}{\partial r} \right|_{T,P,n} = -\frac{2\sigma v_w^\sigma}{r^2} \quad (6)$$

Where v_w is the molecular partial volume of water, r is the radius of the ice drop, and σ is the surface tension of ice.

In figures 7, it is possible to observe different micrographs of frozen loin.

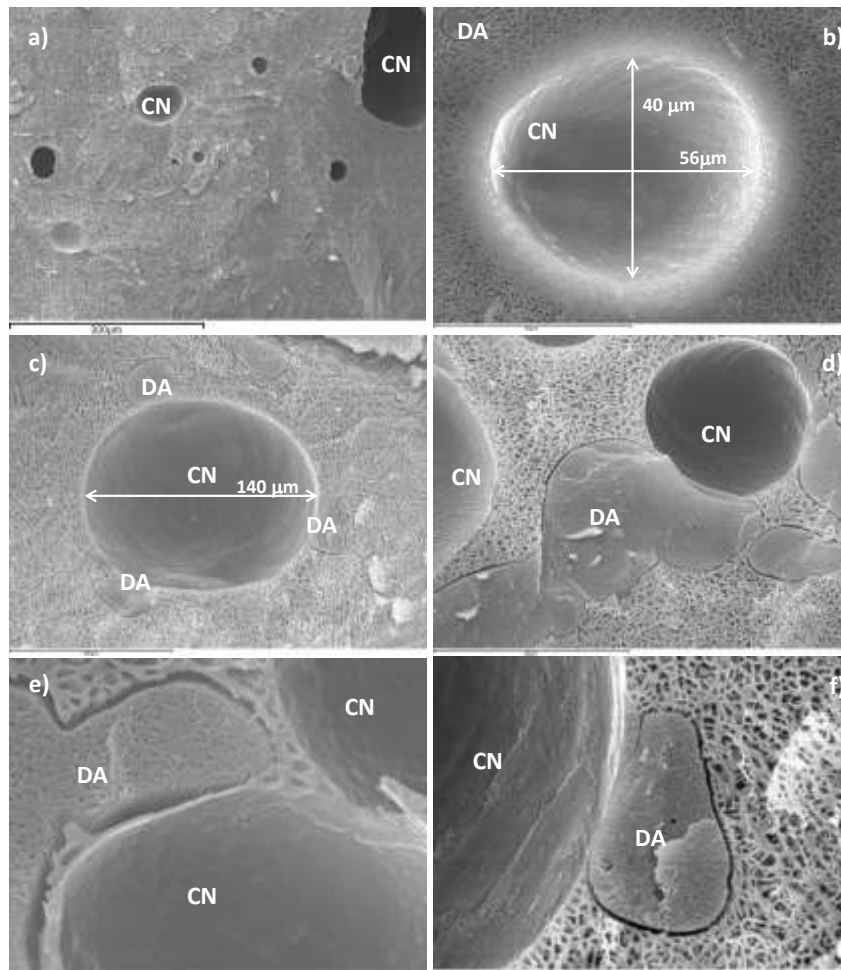


FIGURE 7. Micrograph of frozen pork loin a) 200x, b) 1500x, c) 1000x, d) 1500x, e) 5000x, f) 2000x; where CN (Crystal nucleus), DA (Dried area).

Figure 7a shows a general view of frozen meat with drops of ice agglomerations (CN) shared out by the tissue. Surface tension produces a

decrease of the water chemical potential in the surroundings of crystal nucleus (as equation 6 shows). This phenomenon produces two types of dehydration. The first one is caused by a low flux of water which increases the porosity and preserves the structure, whereas the second one is caused by a fast flux of water that compacts and dehydrates the tissue (DA). This damage is called in the industry "burn".

In figures 7b and 7c, it is possible to observe measured ice agglomerations beside compacted (DA) and high porosity areas. In this case, it can be discerned small and big drops respectively. Micrographs 7d to 7f show the compacted or dehydrated areas in detail.

Figure 8, shows the general impact of water transport throughout the freezing process shown in figure 6. Following the evolution of chemical potential, water flows from the proximity of the lateral (10 mm) to the lateral. In figures 8a and 8g (middle and lateral) it is possible to observe a large number of ice agglomerates spread throughout the tissue. However, in figure 8d (10 mm from lateral) there are very few agglomerates and large dehydrated areas without ice. At the same zone, it is possible to observe in micrograph 8e a big agglomerate surrounded by a porous area.

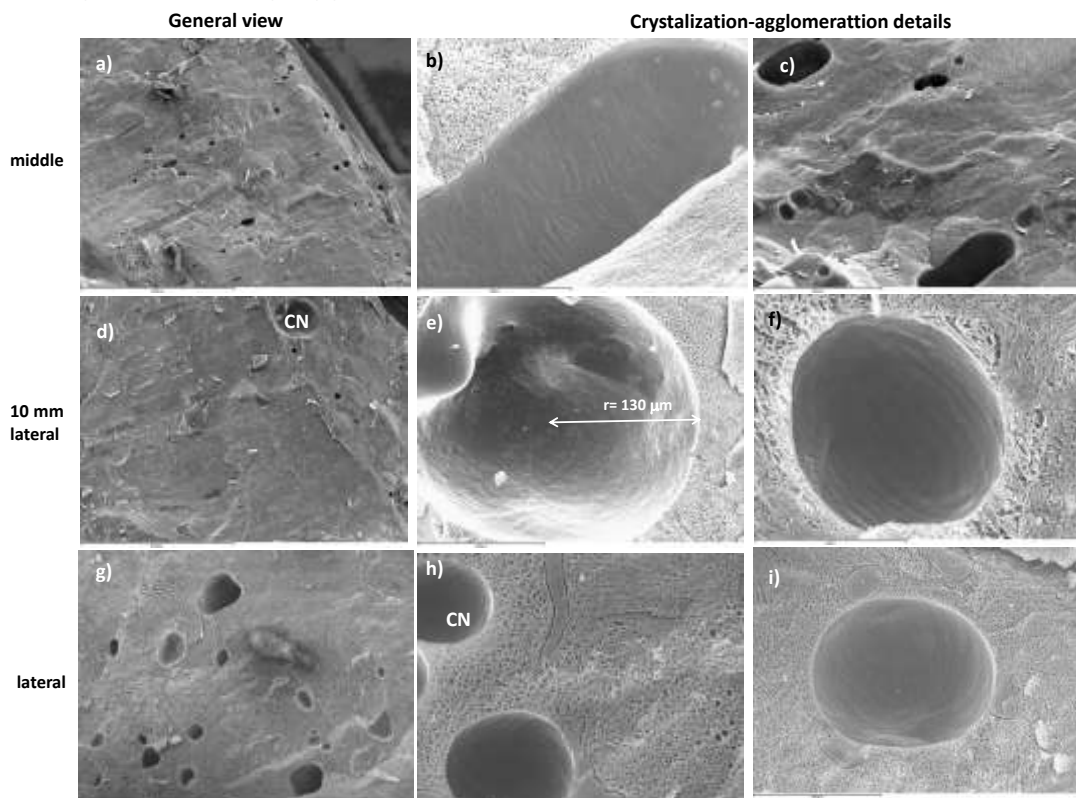


FIGURE 8. Micrograph of frozen pork loin a) 75x, b) 2000x, c) 500x; d) 75x, e) 500x, f) 2000x; g) 200x, h) 1500x, i) 1000x.

3.4 Dielectric properties analysis

Dielectric properties were measured in the fresh and frozen samples in the radiofrequency range and also in the microwave range (Figure 9). The dielectric spectra in the radiofrequency range were measured from 200 Hz to

1 MHz. At these frequencies, the spectrum is the result of different mechanisms involved in the β -dispersion. This dispersion covers all the mechanisms implicated in the orientation of fixed charges in solid surfaces such as membranes or proteins. One of the main effects is called Maxwell-Wagner and it is caused by the solid surface tension. In the figure, it is possible to appreciate that the β -dispersion decreases in the frozen samples mainly due to the fact that the freezing process increases the surface tension but decreases the water mobility.

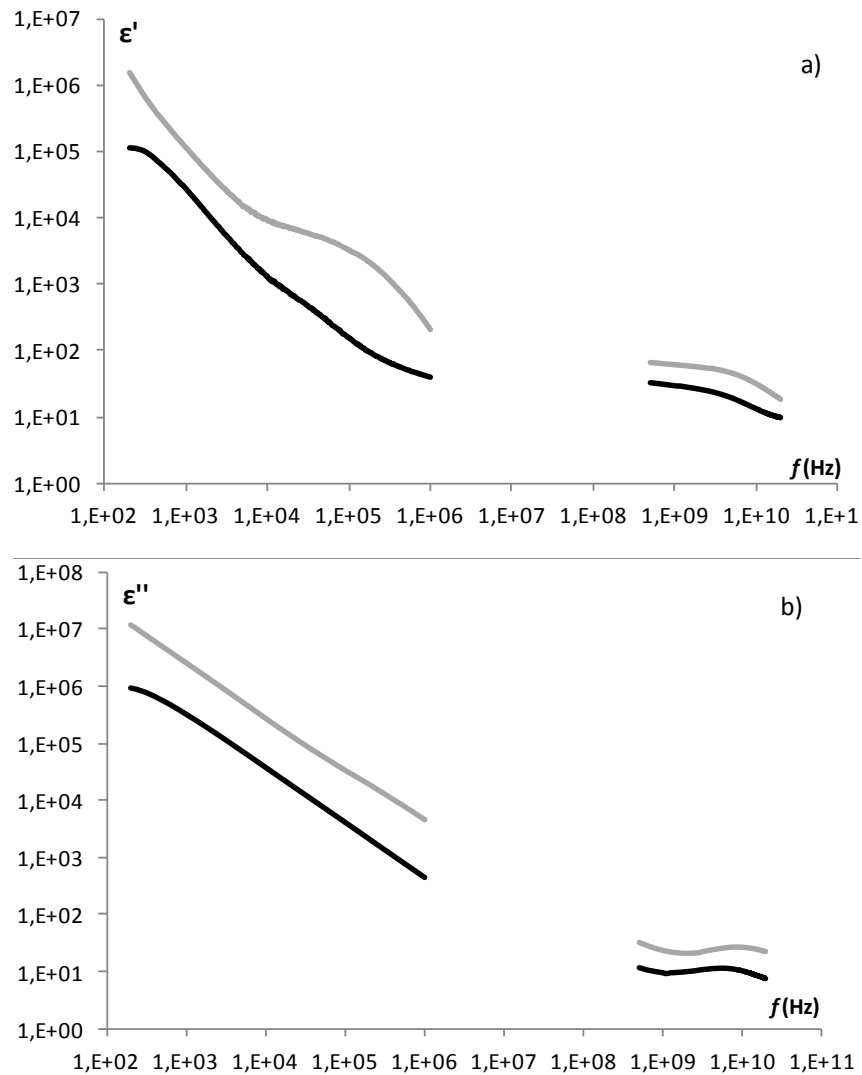


FIGURE 9. a) Dielectric constant spectra and b) dielectric loss factor, where (—) fresh samples and (—) frozen samples.

In order to better understand these phenomena, the loss factor was converted into electric conductivity (Figure 10). It is possible to observe that ions have higher mobility in fresh than in frozen samples (microwave range).

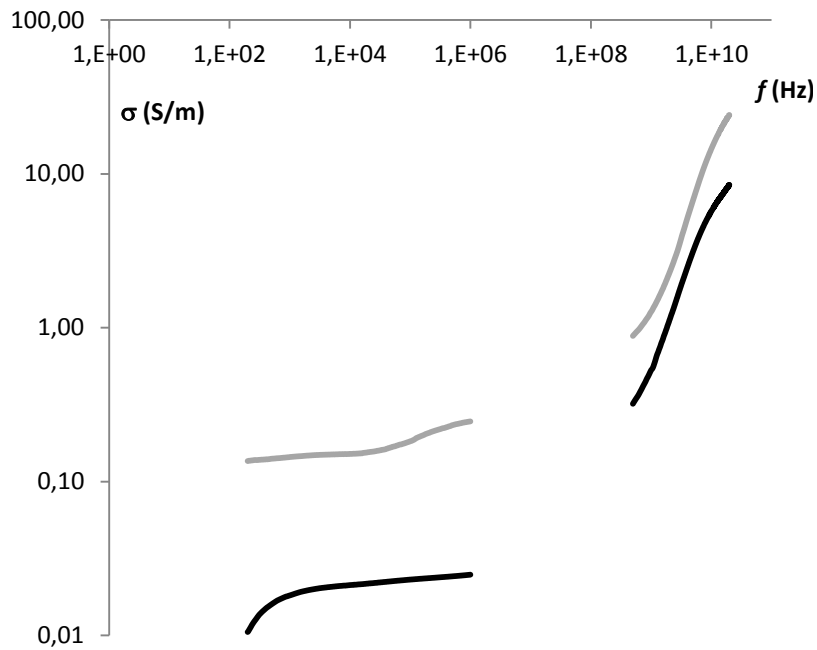


FIGURE 10. Electric conductivity, where (—) fresh samples and (—) frozen samples.

The microwave effect is the result of two mechanisms, dipolar rotation and ionic conductivity. In meat, dipolar rotation is mainly caused by water, which is the most important dipole molecule; in the case of ionic conductivity, there are a wide variety of species with ionic capacity (cations, lactic acid and others). In figure 11, it is possible to appreciate that dielectric constant and loss factor spectra decrease with freezing process due to the decrease in water and ions mobility (ionic strength).

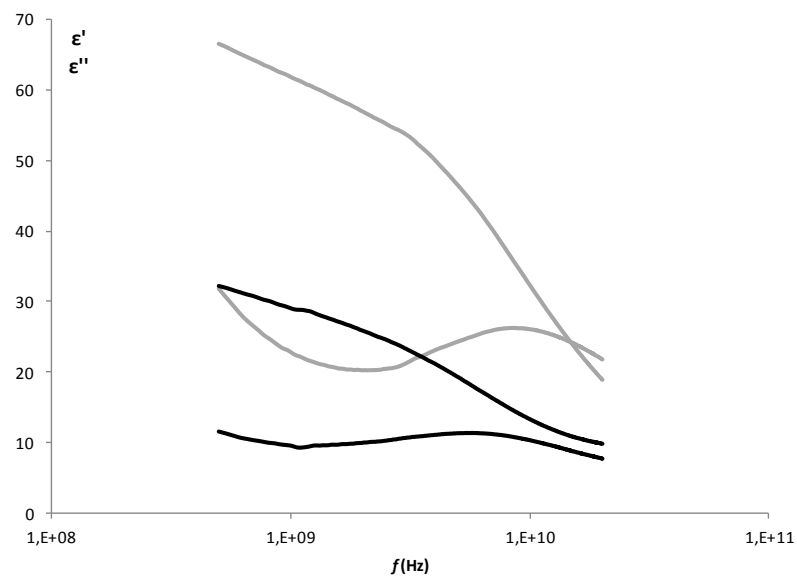


FIGURE 11. Microwave spectra, where (—) fresh samples and (—) frozen samples.

Figure 12 shows the microwave spectra of frozen sample measured at different points of the surface. It is possible to observe that the microwave spectra measured at 10 mm of the lateral decrease with regard to those measured in the middle and lateral of the sample. These measurements confirm that there exists a part of the sample located near the lateral which suffers a higher dehydration.

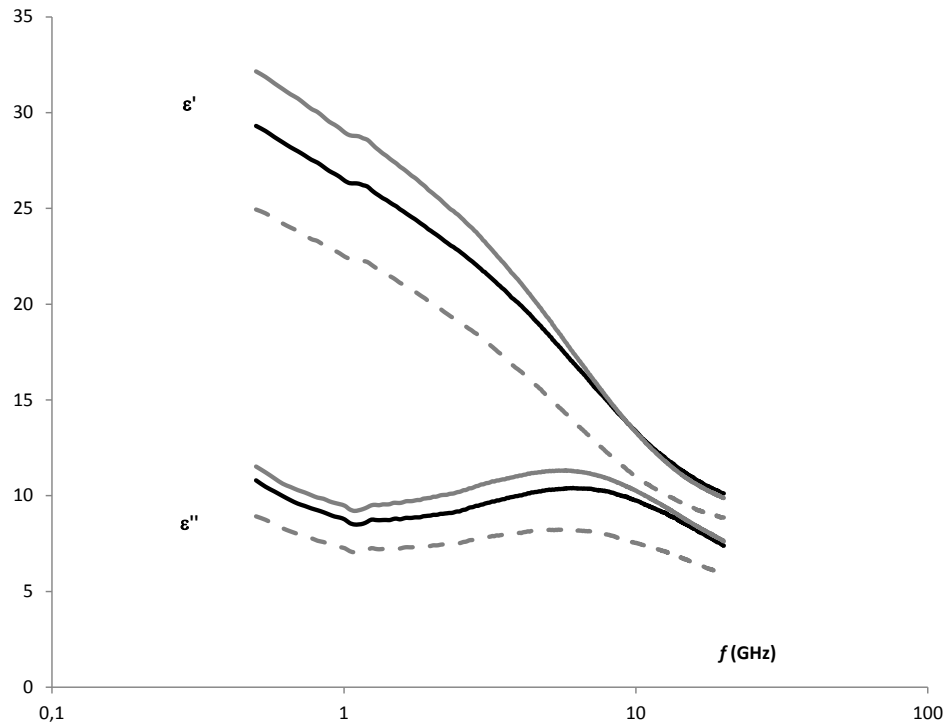


FIGURE 12. Microwave spectra of frozen sample, where (—) frozen lateral (---) frozen at 10 mm from the lateral and (- · -) middle.

4. CONCLUSIONS

Throughout the meat freezing process, the frozen water causes a liquid phase concentration causing a decrease of melting temperature and promoting gradients of water chemical potential. These water chemical potential gradients can be defined at macroscopic and microscopic level. On one hand, at a macroscopic level the water chemical potential depends on the water activity and the temperature. But at a microscopic level, it also depends on the surface tension of ice agglomeration. These mechanisms produce deformation and the breaking of the structure. The dielectric properties confirm that there exists a dehydration near the lateral.

5. REFERENCES

- Alchanatis, V., Cohen, Y., Cohen, S., Moller, M., Meron, M., Tsipris, J., et al. (2006). Fusion of IR and multispectral images in the visible range for empirical and model based mapping of crop water status. *American Society of Agricultural and Biological Engineers*. Paper no. 061171.
- Barassi, C. A., Boeri, R. L., Crupkin, M., Davidovich, L. A., Giannini, D. H., Soulé, C. L., Trucco, R. E., & Lupin, H. M. (1981). The storage life of iced southern blue whiting (*Micromesistius australis*). *Journal of Food Technology*, 16(2), 185–197.
- Burt, J. R., Gibson, D. M., Jason, A. C., & Sanders, H. R. (1976). Comparison of methods of freshness assessment of wet fish. Part III. Laboratory assessments of commercial fish. *Journal of Food Technology*, 11, 117–122.
- Castro-Giraldez, M., Fito, P.J., & Fito, P. (2011). Nonlinear thermodynamic approach to analyze long time osmotic dehydration of parenchymatic apple tissue. *Journal of food engineering*, 1, 34-42.
- Chaerle, L., & Van der Straeten, D. (2000). Imaging techniques and the early detection of plant stress. *Trends in Plant Science*, 5(11), 495-501.
- Clerjon, S., & Damez, J.L. (2007). Microwave sensing for meat and fish structure evaluation. *Meat Science Technology*, 18, 1038-1045.
- Costa, L. N., Stelletta, C., Cannizzo, C., Ganesella, M., Lo fiego, D. P., & Morgante, M. (2007). The use of thermography on the slaughter-line for the assessment of pork and raw ham quality. *International Journal of Animal Science*, 6(1), 704-706.
- Damoglou, A. P. (1980). A comparison of different methods of freshness assessment of herring. In J. J. Connell (Ed.), *Advances in fish science and technology* (pp. 394–399). Farnham, Surrey, UK: Fishing News (Books).
- Delgado, A. E., & Sun, D.W. (2001). Heat and mass transfer models for predicting freezing processes—a review. *Journal of Food Engineering*, 47, 157-274.
- Devine, C. E., Bell, R., Lovatt, S., Chrystall, B. B., & Jeremiah, L. E. (1996). Red meats. In *Freezing Effects on Food Quality*, Jeremiah, L. E. (ed.). Marcel Dekker, New York, pp. 51-84.
- Fennema, O. R., Powrie, W. D., & Marth, E. H. (1973). *Low temperature preservation of foods and living matter*. New York: Marcel Dekker.
- Fito, P. J., Ortolá, M. D., De los Reyes, R., Fito, P., & De los Reyes, E. (2004). Control of citrus surface drying by image analysis of infrared thermography. *Journal of Food Engineering*, 61(3), 287-290.
- Fontan, C.F. & Chirife, J. (1981). The evaluation of water activity in aqueous solutions from freezing point depression. *Journal of Food Technology* 16, 21-30.
- Giorleo, G., & Meola, C. (2002). Comparison between pulsed and modulated thermography in glass-epoxy laminates. *NDT & E International*, 35(5), 287-292.
- Goldstein, R. J., Ibele, W. E., Patankar, S. V., Simon, T. W., Kuehn, P. J., Strykowski, P. J., Tamma, K. K., Heberlein, J. V. R., Davidson, J. H., Bischof, J., Kulacki, F. A., Kortshagen, U., Garrick, S., Srinivasan, V., Ghosh, K., & Mittal, R. (2010). Heat transfer—A review of 2005 literature. *International Journal of Heat and Mass Transfer*, 53, 4397-4447.
- Gowen, A. A., Tiwari, B. K., Cullen, P. J., McDonnell, K., & O'Donnell, C. P. (2010). Application of thermal imaging in food quality and safety assessment. *Trends in Food Science and Technology*, 21, 190-200.
- Hamdami, N., Monteau, J. Y., & Le Bail, A. (2004). Transport properties of a high porosity model food at above and sub-freezing temperatures. Part 1. Thermophysical properties and water activity. *Journal of Food Engineering*, 62, 373-383.
- Hoffmann, A. (1981). The use of the GRTorr meter for the assessment of freshness of iced tropical fish from the Indian Ocean. *Tropical Science*, 23, 283–291.
- Honikel, K.O. (1998). Reference methods for the assessment of physical characteristics of meat. *Meat Science*, 49(4), 447-457.
- Ibarra, J. G., Tao, Y., & Xin, H. (2000). Combined IR imaging-neural network method for the estimation of internal temperature in cooked chicken meat. *Optical Engineering*, 39(11), 3032-3038.
- Ibarra, J. G., Tao, Y., Cardarelli, A. J., & Shultz, J. (2000). Cooked and raw chicken meat: emissivity in the mid-infrared region. *Applied Engineering in Agriculture*, 16(2), 143-148.

- Ibarra, J. G., Tao, Y., Walker, J., &Griffis, C. (1999).Internal temperature of cooked chicken meat through infrared imaging and time series analysis. *Transactions of ASAE*, 42(5), 1383-1390.
- Jie, W., Lite, L. & Yang, D. (2003).The correlation between freezing point and soluble solids of fruits. *Journal of Food Engineering*, 60, 481-484.
- Kent, M., Mackenzie, K., Berger, U.K, Knöchel, R., &Daschner, F. (2000).Determination of prior treatment of fish and fish products using microwave dielectric spectra.*European Food Research Technology*, 210, 427-433.
- Kent, M., Oehlschläger, J., Mierke-Klemeyer, S., Manthey-Karl, M., ,Knöchel, R., &Daschner, F., &Schimmer, O. (2004). A new multivariate approach to the problem of fish quality estimation.*Food Chemistry*, 87, 531-535.
- Lamprecht, I., Schmolz, E., Blanco, L., & Romero, C. M. (2002).Flower ovens: thermal investigations on heat producing plants. *Thermochimica Acta*, 391(1-2), 107-118.
- Lougovois, V. P., Kyranas, E. R., &Kyrana, V. R., (2003).Comparision of selected method os assessing freshness quality and remaining storage life of iced gilthead sea bream (*Spaurusaurata*).*Food Research International*, 36, 551-560.
- Lupin, H. M., Giannini, D. H., Soule, C. L., Davidovich, L. A., &Boeri, R. L. (1980). Storage life of chilled Patagonian hake (*Merluccius hubbsi*).*Journal of Food Technology*, 15(3), 285–300.
- Metaxas, A.C., & Meredith, R.J., 1993. Industrial Microwave Heating. In: IEE Power Engineering Series 4, Peter Peregrinus LTD, London, UK.
- Nelson, S.O., &Datta, A.K., 2001. Dielectric properties of food materials and electric field interactions. In: Datta, A.K., Anantheswaran, R.C. (Eds.), *Handbook of Microwave Technology for Food Applications*. Marcel Dekker, New York, pp. 69– 114.
- Oerke, E. C., Steiner, U., Dehne, H. W., &Lindenthal, M. (2006). Thermal imaging of cucumber leaves affected by downy mildew and environmental conditions. *Journal of Experimental Botany*, 57(9), 2121-2132.
- Rahman, M. S. (2006). State diagram of foods: Its potential use in food processing and product stability. *Trends in Food Science & Technology*, 17, 129-141.
- Rahman, M.S. (1999). Glass transition and other structural changes in foods.In *Handbook of Food Preservation*, Rahman, M.S. (e.d.). Marcel Dekker, Inc., New York, pp: 75-94.
- Rahman, M.S., & Driscoll, R.H. (1994).Freezing points of selected seafoods (invertebrates).*International Food Scienceand Technology*, 29(1), 51-61.
- Rahman, M.S., Machado-Velasco, K. M., Sosa-Morales, M. E., & Velez-Ruiz, J. F. (2008).Freezing Point: Measurement, Data and Prediction. In *Food Properties Handbook*, Rahman, M.S. (e.d.), Taylor & Francis Group, LLC., CRC Press, Boca Ratón, pp: 153-192.
- Rusanov, A. I. (2005). Surface thermodynamics revisited. *Surface Science Reports*, 58(5), 111-239.
- Soyer, A., Özalp, B., Dalmis, U., &Bilgin, U. (2010).Effects of freezing temperature and duration of frozen storage on lipid and protein oxidation in chicken meat. *Food Chemistry*, 120, 1025-1030.
- Stajenko, D., Lakota, M., &Hocevar, M. (2004).Estimation of number and diameter of apple fruits in an orchard during the growing season by thermal imaging.*Computers and Electronics in Agriculture*, 42(1), 31-42.
- Stokes, R. H., & Robinson, R. A. (1965). Interactions in aqueous nonelectrolyte solutions. I. Solute-solvent equilibria. *The Journal of Physical Chemistry*, 70(7), 2126-2131.
- Sugiura, R., Noguchi, N., & Ishii, K. (2007).Correction of low-altitude thermal images applied to estimating soil water status. *Biosystems Engineering*, 96(3), 301-313.
- Toldrá, F. & Flores, M. (2000).The use of muscle enzymes as predictors of pork meat quality.*Food Chemistry*, 69, 387-395.
- Vadivambal, R., &Jayas, D. S. (2011). Applications of termal imaging in Agriculture and Food Industry-A Review.*Food and Bioprocess Technology*, 4(2), 186-199.